ACS Energy LETTERS

Cite This: ACS Energy Lett. 2018, 3, 655−662

PERSPECTIVE

Fundamental Limitations of Wide-Bandgap Semiconductors for Light-Emitting Diodes

Jun Hyuk Park,[†] Dong Yeong Kim,[†] E. Fred Schubert,[‡] Jaehee Cho,[§] and Jong Kyu Kim*[,†]

[†]Department of Materials Science and Engineering, Pohang University of Science and Technology, 77 Cheongam-Ro, Nam-Gu, Pohang, Gyeongbuk 37673, Republic of Korea

[‡]Department of Electrical, Computer, and Systems Engineering, Rensselaer Polytechnic Institute, 110 Eighth Street, Troy, New York 12180, United States

[§]School of Semiconductor and Chemical Engineering, Semiconductor Physics Research Center, Chonbuk National University, Jeonju 54896, Republic of Korea

ABSTRACT: **Fundamental limitations of wide-bandgap semiconductor devices are caused by systematic trends of the electron and hole effective mass, dopant ionization energy, and carrier drift mobility as the semiconductor's bandgap energy increases. We show that when transitioning from narrow-bandgap to wide-bandgap semiconductors the transport properties of charge carriers in pn junctions become increasingly asymmetric and characterized by poor p-type transport. As a result, the demonstration of viable devices based on bipolar carrier transport, such as pn junction diodes, bipolar transistors, light-emitting diodes (LEDs), and lasers, becomes increasingly difficult or even impossible as the bandgap energy increases. A systematic analysis of the efficiency droop in LEDs is conducted for room temperature and cryogenic temperature and for emission wavelengths ranging from the infrared, through the visible (red and blue), to the deep-ultraviolet part of the spectrum. We find that the efficiency droop generally increases with bandgap energy and at cryogenic temperatures. Both trends are consistent with increasingly asymmetric carrier-transport properties and increasingly weaker hole injection as the bandgap energy of LEDs increases, indicating that fundamental limitations of wide-bandgap semiconductor devices are being encountered.**

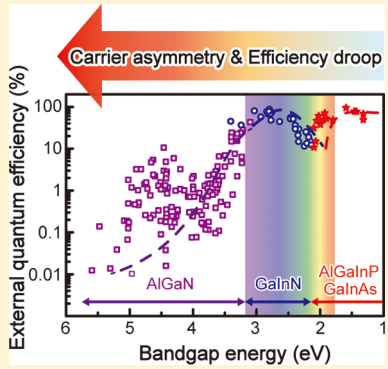

During the past 100 years, inorganic light-emitting diodes (LEDs) have undergone a significant evolution, from the very first visible LED based on SiC to today's highly efficient white LEDs, that resulted from a series of breakthroughs and advances in epitaxial growth of high-quality crystals, the employment of heterostructures, and advances in device architecture such as improved light out-coupling.[1] Semiconductor material systems used for LEDs covering the visible spectrum include III-phosphides (AlGaInP) that are capable of emitting red, orange, amber, and yellow light and III-nitrides (AlGaInN) for emitting green, cyan, blue, and violet light as well as ultraviolet (UV) radiation. LEDs are being used in areas as diverse as indicators, signage, displays, and general lighting. Furthermore, using efficient GaInN-based blue LEDs in combination with a phosphor has enabled bright and energy-saving white light sources.[2,3] Tremendous progress has been made, as demonstrated by white LEDs with a greater than 200 lm/W efficacy, far exceeding the efficacy of traditional incandescent and Hg-discharge-based fluorescent lighting devices. The future of white LEDs looks bright and is flourishing, considering emerging and advanced applications such as smart and adaptive lighting sources, visible light communication, and purification and disinfection using light sources that are pleasant, healthy, and energy efficient.[3,4]

A strong asymmetry between n-type and p-type properties, such as doping concentration, carrier injection, effective mass, and carrier mobility, would pose a fundamental challenge to the efficiency of LEDs.

In an LED, a light quantum (photon) is generated when an electron in the conduction band radiatively recombines with a hole in the valence band. Because radiative transitions in a semiconductor are from the conduction band minimum to the valence band maximum, the energy of the photon is approximately equal to the bandgap energy of the semiconductor. Quantum wells, frequently composed of two alloy semiconductors whose bandgap is tuned by varying the alloy composition, enable good confinement for electrons and holes to the active region while emitting the desired color for light. It is apparent that the efficiency of an LED hinges on electrons

Received: January 1, 2018
Accepted: February 13, 2018
Published: February 13, 2018

DOI: 10.1021/acsenergylett.8b00002
ACS Energy Lett. 2018, 3, 655−662

and holes being injected into the quantum well active region. In other words, a strong asymmetry between n-type and p-type properties, such as doping concentration, carrier injection, effective mass, and carrier mobility, would pose a fundamental challenge to the efficiency of LEDs. Indeed, there is a pronounced trend in LED efficiency: As the bandgap energy increases, i.e., as the wavelength becomes shorter, the external quantum efficiency (EQE) of LEDs generally decreases; furthermore, the efficiency droop problem becomes more severe.

In this Perspective, we first discuss the fundamental trends of the asymmetric carrier transport properties in terms of electron and hole effective mass, dopant ionization energy, dopant ionization, and carrier drift mobility as the semiconductor's bandgap energy increases. We then show a wide range of experimental results of high-quality GaAs infrared (IR) LEDs, AlGaInP red LEDs, GaInN blue LEDs, and AlGaN deep-ultraviolet (DUV) LEDs. It is found that the efficiency droop increases with the semiconductor's bandgap energy, consistent with increasingly asymmetric carrier-transport properties as well as increasingly weaker hole injection as the bandgap energy of LEDs increases. As the asymmetry in carrier transport increases, the portion of electron current in the p-type semiconductor layer to the total LED current becomes larger due to increasing electron overflow, which results in the decrease of hole current in the p-type region and hence the hole injection into the multiple quantum well (MQW). Therefore, pn junction based wide-bandgap semiconductor devices would be severely limited by fundamental p-type doping limitations.

Figure 1 shows reported EQEs of GaAs IR, AlGaInP and GaInN visible, and AlGaN UV LEDs as a function of emission

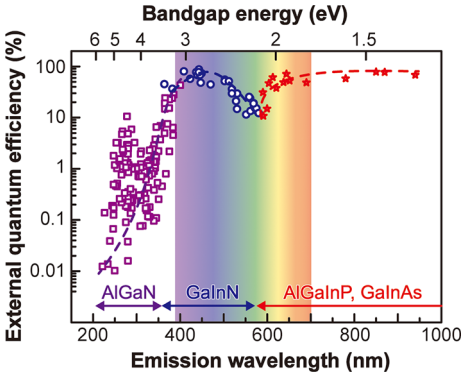

Figure 1. EQEs of AlGaInP- and GaInAs-based IR and GaInN-based visible and AlGaN-based UV LEDs as a function of emission wavelength, as reported in the technical literature.[5−8] External quantum efficiencies of 780, 870, and 940 nm IR LEDs were estimated through the operation current and light output power of commercially available unmounted LEDs.

wavelength, i.e., bandgap energy of the semiconductor.[5−8] In the IR and visible regions, efficiencies are generally high, that is, greater than 50%. In the center of the visible region, a dip in the efficiency occurs that is known as the "green gap". The green gap is well understood for both material systems, AlGaInP and GaInN. As the Al content of AlGaInP increases, thus, the emission wavelength becomes green and the energy band structure of AlGaInP undergoes a transition from direct to indirect,[1] resulting in a rapidly reduced quantum efficiency. Meanwhile, as the In content of GaInN increases for green emission, compositional fluctuation (In clustering) occurs, inducing spatial separation between the electron wave function and hole wave function,[6] which makes radiative recombination inefficient. Inspection of the figure also reveals that there is a significant problem in the UV where the LED efficiency decreases from >50% at the visible/UV boundary to values as low as 0.01−10% at 200−300 nm. The poor efficiency in the DUV is a clear indicator of a fundamental limitation encountered with wide-bandgap semiconductors.

First, we discuss a fundamental trend in asymmetric carrier transport properties in semiconductors as the bandgap energy increases or the temperature decreases. The two-band Kane model, based on the quantum-mechanical $k \cdot p$ perturbation theory,[10] allows for the identification of general trends in the field of semiconductors.[9] The model predicts a specific dependence of the electron effective mass on the semiconductor's bandgap energy, E_g. The electron effective mass can be expressed as follows[10]

$$\frac{m_e}{m_e^*} = 1 + \frac{2}{m_e E_g} |\langle \nu | p_x | c \rangle|^2 \quad (1)$$

where m_e is the free electron mass, m_e^* is the electron effective mass in the semiconductor, p_x is the momentum operator in the x direction, $|c\rangle$ is the state at the conduction band minimum, and $|\nu\rangle$ is the light-hole state at the valence band maximum.[10]

Let us consider two limiting cases of the bandgap energy: First, consider a narrow-gap semiconductor or even a semiconductor with vanishingly small bandgap energy, i.e., $E_g \rightarrow 0$. In this case, the right-hand side of eq 1 becomes very large so that m_e^* approaches zero. This trend is confirmed by experimental values of m_e^* with narrow-direct-bandgap III−V semiconductors (for example, InAs, with $E_g = 0.354$ eV, has an effective mass of $m_e^* = 0.022 m_e$), and on the extreme side, graphene has a zero bandgap energy ($E_g = 0.0$ eV) as well as a zero effective mass ($m_e^* = 0.0 m_e$) near the Dirac point.[11] Second, consider wide-bandgap semiconductors. For the limit of large-bandgap energies, the right-hand side of eq 1 approaches 1.0, and thus, $m_e^* \approx m_e$. This trend is consistent with experimental values of m_e^* of wide-direct-bandgap III−V semiconductors: For example, AlN ($E_g = 6.28$ eV) has the largest electron effective mass among binary direct-gap III−V semiconductors ($m_e^* = 0.33 m_e$).[12] Accordingly, eq 1 predicts the theoretical trend that the electron effective mass increases as E_g increases, consistent with the well-known experimental values of m_e^* of actual semiconductors.

Additional guidance on the effective masses can be obtained from the Kronig−Penney model that is based on quantum mechanics considering the propagation of electrons in a one-dimensional potential,[13] which allows valuable insight into the carrier transport in semiconductors. Within the framework of the Kronig−Penney model, electrons in lower-lying bands are necessarily subject to higher potential barriers and thus become more spatially localized than electrons in higher-lying bands. The stronger localization manifests itself as a heavier electron effective mass associated with lower bands. As a result, valence band carriers (holes) fundamentally have a heavier effective mass than conduction band carriers (electrons).

We note that although the Kronig−Penney model gives useful guidance, the model is limited to one dimension and thus is an oversimplification of the actual 3D crystal potential. Despite the oversimplification, experimental values for the hole effective mass generally follow the predicted theoretical trend. For example, direct-gap semiconductors such as GaAs, GaInN,

DOI: 10.1021/acsenergylett.8b00002
ACS Energy Lett. 2018, 3, 655−662

GaN, and AlN consistently have a hole effective mass that is heavier than the electron effective mass. Taken together, the two-band Kane model and Kronig–Penney model indicate that as the bandgap energy E_g of semiconductors increases, so does the electron mass and even more so does the heavy hole effective mass.

Taken together, the two-band Kane model and Kronig–Penney model indicate that as the bandgap energy E_g of semiconductors increases, so does the electron mass and even more so does the heavy hole effective mass.

The hydrogen-atom model (effective mass model) relates the electron and hole effective mass to the donor and acceptor ionization energy, respectively.[14] As concluded from the effective mass trends and the hydrogen-atom model, the donor ionization energy and particularly the acceptor ionization energy increase as the bandgap energy increases. Because the degree of dopant ionization depends exponentially on the dopant ionization energy, a slightly larger acceptor ionization energy (than the donor ionization energy) can result in a much lower degree of acceptor ionization (than donor ionization). Furthermore, the effective mass affects not only the dopant ionization but also the carrier drift mobility by means of the Drude equation $\mu = e\tau/m^*$, where μ is the mobility and e, τ, and m^* are the elementary charge, the average time between collisions (scattering time), and the carrier effective mass, respectively. Finally, the above-described trends indicate that pn junctions made of narrow-bandgap semiconductors enjoy full ionization of donors and acceptors, whereas pn junctions made of wide-bandgap semiconductors suffer from a lack of full ionization, particularly for acceptors. Note that the discussion in the present paper can be applied to elemental semiconductors, as well as compound semiconductors. The range of bandgap energy includes Ge and Si (0.66 and 1.12 eV) III–V arsenides (typically 0.5 to 2.0 eV), III–V phosphides (typically 1.0 to 2.5 eV), and III–V nitrides (typically 2.5 to 6.0 eV). Although these are diverse semiconductor materials, we believe that the Kane model, the Kronig–Penney model, and the effective mass model can be applied to these semiconductors.

The above-described trends indicate that pn junctions made of narrow-bandgap semiconductors enjoy full ionization of donors and acceptors, whereas pn junctions made of wide-bandgap semiconductors suffer from a lack of full ionization, particularly for acceptors.

The conclusions drawn from the models discussed above are well matched by experimental values of effective masses and ionization energies. Figure 2 shows the effective mass of electrons and holes and the dopant ionization energy as a function of the bandgap energy of semiconductors, as gathered from the technical literature.[15–25] As summarized in Figure 2, the narrow-bandgap GaAs material system (operating at IR

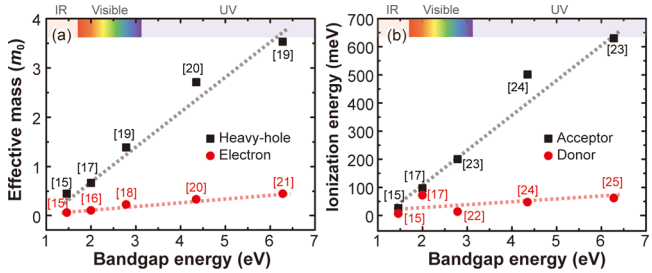

Figure 2. (a) Variation of electron and heavy-hole effective masses with the energy bandgap of semiconductors. (b) Dopant ionization energy as a function of the bandgap energy of different direct-gap III–V semiconductors.[15–25]

wavelengths) with its low dopant activation energies ($E_d < kT$; $E_a \approx kT$ at 300 K; $p \approx N_A$; $n \approx N_D$; and $p \approx n$) enjoys full dopant activation, where E_d and E_a are the donor and acceptor ionization energy, k and T are the Boltzmann constant and the absolute temperature, p and n are the hole and electron concentration, and N_A and N_D are the acceptor and donor concentration, respectively. Although the trend of increasing effective masses is similar for electrons and holes, the effect on electrons is not as severe as that for holes, as shown in Figure 2b. The AlGaInP material system (operating at red to yellow wavelengths) has required thick current-spreading layers due to its low p-type conductivity.[26] The GaInN material system (operating at green to violet wavelengths) is well-known for its p-type doping problem.[27,28] Finally, the AlGaN material system (operating at near-UV and DUV wavelengths) is known to have a severe p-type doping problem (even more so than the GaInN material system) with $E_a \gg E_d$; $p \ll N_A$; $p \ll n$; and $\mu_p \ll \mu_n$.[29–31] Accordingly, the above-discussed theoretical trends are closely replicated in the GaAs (IR), AlGaInP (red), GaInN (blue), and AlGaN (DUV) material systems. What are the consequences of these trends? As E_g increases, pn junctions suffer from increasingly asymmetric carrier-transport properties of the n-type side (higher ionization) and p-type side (very low ionization), resulting in an imbalanced carrier concentration in the active region of LEDs.

What are the consequences of these trends? As E_g increases, pn junctions suffer from increasingly asymmetric carrier-transport properties of the n-type side (higher ionization) and p-type side (very low ionization), resulting in an imbalanced carrier concentration in the active region of LEDs.

Next, we present a wide range of experimental results showing a strong correlation between asymmetric carrier transport, bandgap energy, and efficiency droop by comparing four different types of commercialized LEDs: IR (OSRAM), red (OSRAM), blue (Korean Photonics Technology Institute, KOPTI), and DUV LED (Rayvio). High-quality commercial GaAs IR LEDs with the peak wavelength, λ_{peak}, of 850 nm, AlGaInP red LEDs (λ_{peak} = 620 nm), GaInN blue LEDs (λ_{peak} = 450 nm), and AlGaN DUV LEDs (λ_{peak} = 280 nm) were utilized, all of which were grown by metal–organic chemical vapor deposition. The IR LED employs a 40 period GaAs/

DOI: 10.1021/acsenergylett.8b00002
ACS Energy Lett. 2018, 3, 655–662

AlGaAs MQW active region, while the red LED has a 38 period AlGaInP/AlInP MQW active region. Both blue and DUV LEDs employ a 5 period GaInN/GaN and AlGaN/AlGaN MQW active region, respectively. The chip size is 0.2 × 0.2 mm^2 for the GaAs IR LED, 0.7 × 0.7 mm^2 for the AlGaInP red LED, 1.1 × 1.1 mm^2 for the GaInN blue LED, and 2 × 2 mm^2 for the AlGaN DUV LED. Light output−current−voltage (L−I−V) characteristics were measured at temperatures ranging from 80 to 300 K using a vacuum chamber probe station equipped with an Agilent B2902A precision source-measurement unit. The light output was collected by a UV-enhanced Si photodiode. All LEDs were operated under pulsed injection currents (pulse period = 5 ms, duty cycle = 0.5%) in order to avoid self-heating effects.

Figure 3a shows I−V curves of four types of LEDs measured at temperatures ranging from 80 to 300 K with a 20 K interval.

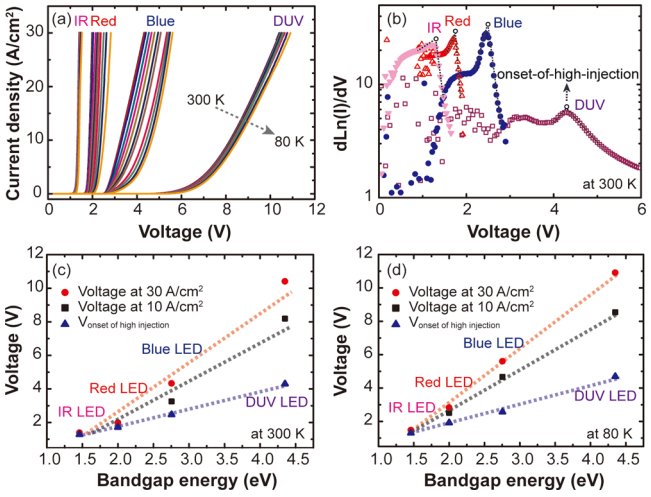

Figure 3. (a) I−V characteristics of the GaAs IR LED, AlGaInP red LED, GaInN blue LED, and AlGaN DUV LED measured at temperatures ranging from 80 to 300 K. (b) d ln(I)/dV versus V plot used to identify the onset voltage at high injection, which is the transition point from low injection to high injection. Variation of the forward voltage with bandgap energy of semiconductors at (c) 300 and (d) 80 K.

The figure shows variations with bandgap energy and temperature of the turn-on voltage and series resistance. When the applied voltage approaches the built-in voltage V_{bi}, semiconductor pn junctions enter the high-injection regime. The V_{bi} is given by $V_{bi} = (kT/e)\ln(N_A N_D/n_i^2) \approx (kT/e)\ln(p_{p0}n_{n0}/n_i^2)$, where n_i is the intrinsic carrier concentration.[1] Figure 3b shows a 300 K d ln(I)/dV plot as a function of current showing a clear transition point from the low-injection to the high-injection regime.[32] The onset voltage point for high injection is determined by using the point where the d ln(I)/dV versus V plot has a maximum, as shown in Figure 3b. Figure 3c,d shows the variation in the onset-of-high-injection and forward operating voltages of the LEDs for two current densities (10 and 30 A/cm^2) as a function of bandgap energy at 300 K. The onset-of-high-injection voltage increases (approximately linearly) from 1.28 V in the IR LED to 4.29 V in the DUV LED. As a pn junction becomes increasingly asymmetric (as p_{p0} becomes much smaller than n_{n0}), V_{bi} decreases (relative to E_g/e) and, consequently, so does the onset voltage of high injection. That is, as E_g increases, (i.e., increasingly asymmetric condition), so more does $E_g - eV_{bi}$, and the diodes become increasingly prone to high-injection phenomena, as apparent from Figure 3.

What does this mean for LEDs? LEDs, in order to obey energy conservation, have a forward operating voltage of E_g/e, as confirmed experimentally for IR and red, blue, and DUV LEDs (where E_g is the bandgap energy of the active region). The experimentally measured voltages at 10 and 30 A/cm^2 gradually increase with increasing bandgap energy, as shown in Figure 3c,d. However, the forward voltage measured at 10 and 30 A/cm^2 varies more rapidly than the onset-of-high-injection voltage. This necessarily means that LEDs, as E_g increases, are more prone to operating in the high-injection regime. When the applied forward voltage is higher than the onset-of-high-injection voltage, the incremental voltage will drop across the most resistive part of the p-type region, i.e., the electron-blocking layer (EBL) that is typically grown on the MQW active region to prevent the injected electrons from escaping out of the active region. Accordingly, the effectiveness of the EBL is compromised in the high-injection regime so that electrons leak out of the MQW active region. Consequently, electron overflow can be significant despite of the potential barrier induced by EBL, resulting in the efficiency droop.[32] This reasoning suggests that the efficiency droop is correlated with the bandgap energy of semiconductors. The efficiency droop is a widely discussed phenomenon in LEDs, particularly in AlGaInP-based, GaInN-based, and AlGaN-based LEDs.[33−36] There have been competing explanations for the predominant cause of the droop, such as Auger recombination, defect-

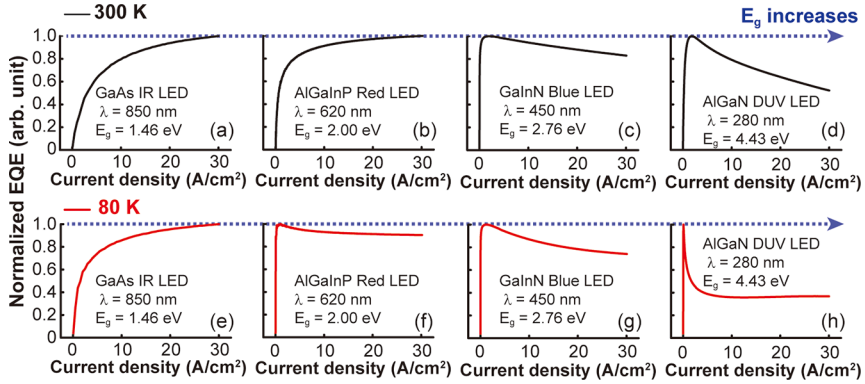

Figure 4. Normalized EQE curves as a function of current density for a (a) GaAs IR LED, (b) AlGaInP red LED, (c) GaInN blue LED, and (d) AlGaN DUV LED measured at 300 K and (e−h) the same set of LEDs measured at 80 K.

DOI: 10.1021/acsenergylett.8b00002
ACS Energy Lett. 2018, 3, 655−662

assisted Shockley–Read–Hall (SRH) recombination, lack of hole injection, and/or leakage of electrons from the active region.[34,37−39] All of them could cause the efficiency droop. However, among a variety of causes of the efficiency droop, it has been postulated that the efficiency droop is mainly associated with a lack of hole injection.[40−42] Each hole not injected into the active region is necessarily equivalent to one electron leaking out of the active region. Accordingly, lack of hole injection and electron leakage are "two sides of the same coin", i.e., two interrelated aspects of the same phenomenon. Therefore, we investigate the correlation between the efficiency droop and the bandgap energy and further the lack-of-hole-injection effect on the efficiency droop for LEDs consisting of multiple semiconductors having bandgap energies that correspond to IR, red, blue, and UV wavelengths. Given the theoretical prediction and supporting experimental results, the authors believe that the lack of efficient hole transport in $Al_xGa_{1-x}N$ ($x > 0.5$) and SiC[43] and the complete lack of hole transport in very wide bandgap semiconductors, such as AlN and C (diamond),[44] are fundamental in nature and would be extremely difficult to overcome.

Figure 4 shows normalized EQE curves for the four different types of LEDs as a function of current density measured at 300 and 80 K, respectively. At room temperature (300 K), the GaAs IR LED and AlGaInP red LED do not show the efficiency droop at current densities up to 30 A/cm^2, while the GaInN blue LED and AlGaN DUV LED show a moderate and strong efficiency droop of 16.9 and 48.5%, respectively. At cryogenic temperature (80 K), the efficiency droop is still not observed in the GaAs IR LED (with narrow E_g), while the efficiency droop for the AlGaInP red LED, GaInN blue LED, and AlGaN DUV LED are more pronounced with values of 9.75, 25.84, and 63.3%, respectively.

Figure 5 shows a summary of the variation of the efficiency droop at 30 A/cm^2 for the four different LEDs as a function of the energy bandgap at 300 and 80 K. We find that the magnitude of efficiency droop systematically increases with the bandgap energy at both room and cryogenic temperatures. As E_g increases, the acceptor ionization energy increases more strongly than the donor ionization energy, resulting in increasingly asymmetric carrier concentration and injection. In addition, the difference in electron and hole mobilities increases as E_g increases. Regardless of the amount of quantitative contribution of concentration and mobility at this moment, both n- and p-type carrier concentrations and their transport characteristics become increasingly asymmetric when going from narrow- to wide-bandgap materials. Furthermore, the magnitude of efficiency droop increases at cryogenic temperatures for all LEDs. This trend can be readily understood by the exacerbation of the asymmetry of carrier transport at cryogenic temperatures. As the temperature is lowered to cryogenic temperatures, holes freeze out onto acceptor states, so that the imbalance between electron and hole transport increases even further. It is the lack of hole transport and lack of hole injection that exacerbate the efficiency droop at cryogenic temperatures. Therefore, the efficiency droop, when considered for a range of semiconductor materials and temperatures, is supported by the asymmetric transport characteristics as the cause. We point out that both trends (with respect to E_g and T) are consistent with hole injection becoming increasingly difficult as E_g increases and T decreases. We note that both trends have not been shown to be consistent with other mechanisms that have been suggested for the efficiency droop in the technical literature. For example, Auger recombination would be expected to be more pronounced in low-bandgap semiconductors and at higher temperatures, contrary to the experimental results.[45] The results presented above along with the analysis of the underlying causes allow for a coherent understanding of the efficiency droop in a wider context, including its dependence on bandgap energy and temperature.

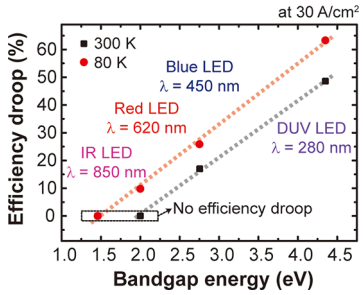

Figure 5. Variation of efficiency droop with bandgap energy for semiconductors with emission wavelengths ranging from IR to DUV.

> Both n- and p-type carrier concentrations and their transport characteristics become increasingly asymmetric when going from narrow- to wide-bandgap materials.

Next, let us discuss potential ways to overcome the limitations for wide-bandgap bipolar semiconductors, particularly LEDs. Despite the challenges originating from intrinsic material properties of wide-bandgap materials, especially AlGaN, sustained research efforts in the development of LEDs have advanced the EQE of UV LEDs through refined epitaxial growth techniques (including pulsed atomic-layer epitaxy[46,47] and high-temperature growth[48]), as well as stress-managing techniques that result in a strongly reduced defect density.[49,50] As discussed above, another critical area that is in need of a major improvement is p-type doping. In a conventional way, a p-type GaN layer grown on a p-type AlGaN layer is used for a metal-contact and a hole-supplying layer to overcome low p-doping problem, but it causes a strong absorption of emitted UV photons by the p-type GaN, thus leading a poor light-extraction efficiency. One of the potential ways to achieve a highly conductive p-type wide-bandgap material is to grow superlattices that have been shown to enhance the free hole concentration in AlGaN.[51−54] The energy band modulation of superlattices along with the modulation caused by the polarization fields enables a higher acceptor ionization ratio and thus a higher hole concentration. Similarly, Al-composition-graded AlGaN is a promising method for inducing mobile hole gases by utilizing a built-in polarization-induced electrical field in the bulk Al-graded layer, which can facilitate ionization of deep acceptor dopants.[23,55] Another proposed alternative to overcome the p-type doping problem is introduction of a polarization-charge-enhanced tunnel junction (PCE-TJ).[56,57] The polarization charge at heterointerfaces of a tunnel junction can enable interband tunneling by inducing

DOI: 10.1021/acsenergylett.8b00002
ACS Energy Lett. 2018, 3, 655−662

strong band bending without heavily doped semiconductor layers. Therefore, holes can be injected into the active layer without a p-type doped AlGaN layer with PCE-TJ. On the other hand, LEDs with a thick QW for a large active volume have been suggested to solve the problems that can be caused by increased carrier density such as Auger recombination.[58] Nonpolar or semipolar nitride-based LEDs[59−61] would be effective to enable thick QW structures by alleviating the quantum-confined Stark effect caused by the polarization field.

Recently, light-extraction-enhancing approaches have been proposed, including a combination of a UV-transparent p-type AlGaN layer and UV-reflective metal contact,[62] use of photonic crystals,[63] and sidewall-emission-enhancing structures to utilize the inherently strong TM-polarized light emitted from the AlGaN active region.[64−66]

The efficiency droop, when considered for a range of semiconductor materials and temperatures, is supported by the asymmetric transport characteristics as the cause.

In conclusion, inorganic LEDs have undergone a significant evolution that resulted from a series of breakthrough advances to enable bright and energy-saving lighting sources that far exceed the efficiency of traditional lighting sources. In this Perspective, we employed the two-band Kane model, the Kronig−Penney model, and the hydrogen-atom model to show that as the bandgap energy increases so does the electron effective mass and even more so the heavy-hole effective mass. Consequently, (i) the donor and particularly the acceptor ionization energies become larger as E_g increases and (ii) the electron mobility and particularly the hole mobility become lower as E_g increases. These theoretical trends are fully consistent with established experimental values of the effective masses, ionization energies, and mobilities in semiconductors with bandgap energies ranging from the IR through the visible to the DUV. The increasingly asymmetric carrier transport makes hole injecting increasingly difficult as E_g increases and as T decreases. As a consequence, the LEDs' onset voltage for high injection becomes increasingly lower when compared to the forward operating voltage, demonstrating that LEDs increasingly operate in the high-injection regime as E_g increases. We also investigated the efficiency droop in LEDs with bandgap energies ranging from the IR to the DUV. We found the following systematic trends: the magnitude of the efficiency droop increases with E_g and at cryogenic temperatures, consistent with hole injection in pn junction LEDs becoming increasingly difficult as E_g increases and T decreases. The trends with respect to temperature and bandgap energy are highly systematic for the entire range of LEDs investigated (IR, red, blue, and DUV). The results show that a wide-bandgap semiconductor LED is subject to fundamental limitations with the efficiency droop's highly systematic dependence on E_g and T, as demonstrated for LEDs made of a wide range of semiconductor materials, being a manifestation of these fundamental limitations. Despite such challenges originating from intrinsic material properties of wide-bandgap semiconductors, impressive research efforts are being made to overcome the limitations, enhancing internal quantum efficiency, light-extraction efficiency, and hence EQE.

AUTHOR INFORMATION

Corresponding Author

*E-mail: kimjk@postech.ac.kr.

ORCID

Dong Yeong Kim: 0000-0003-0365-7668
Jaehee Cho: 0000-0002-8794-3487
Jong Kyu Kim: 0000-0003-1643-384X

Notes

The authors declare no competing financial interest.

Biographies

Jun Hyuk Park received the Ph.D. degree in Materials Science and Engineering at Pohang University of Science and Technology (POSTECH), Pohang, South Korea in 2017. His main research is about efficiency droop phenomena in III-nitride LEDs. Currently, he works as a senior engineer at LED business division in Samsung Electronics Co., South Korea since 2017.

Dong Yeong Kim is a Ph.D. candidate at Pohang University of Science and Technology (POSTECH). His research focuses on nitride semiconductors and their optoelectronic applications including the wurtzite AlInGaN material system and two-dimensional hexagonal boron nitride (h-BN).

E. Fred Schubert made pioneering contributions to the field of compound semiconductor materials and devices, particularly to the doping of compound semiconductors and to the development and understanding of LEDs. He is currently a professor in the Department of Electrical, Computer, and Systems Engineering, Rensselaer Polytechnic Institute in Troy, New York, U.S.A.

Jaehee Cho is a scientist in the field of photonics materials and devices with more than 15 years of academic and industrial experience. He has made significant contributions to the field of GaN-based photonics. Now he is an assistant professor in the Department of Semiconductor Science and Technology, Chonbuk National University, Jeonju, Republic of Korea.

Jong Kyu Kim is a professor in the Department of Materials Science and Engineering at POSTECH. He has made pioneering contributions to the fields of AlGaInN-based light-emitting diodes and future smart lighting applications.

ACKNOWLEDGMENTS

The Authors gratefully acknowledge support by the Brain Korea 21 PLUS project for Center for Creative Industrial Materials (F14SN02D1707) and by the development of R&D professionals on LED convergence lighting for shipbuilding/marine plant and marine environments (Project No: N0001363) funded by the Ministry of Trade, Industry & Energy (MOTIE) of Korea.

REFERENCES

(1) Schubert, E. F. In *Light-Emitting Diodes*, 2nd ed.; Schubert, E. F., Eds.; Cambridge University Press: Cambridge, U.K., 2006.

(2) Nakamura, S. Nobel Lecture: Background story of the invention of efficient blue InGaN light emitting diodes. *Rev. Mod. Phys.* **2015**, *87*, 1139−1151.

(3) Cho, J.; Park, J. H.; Kim, J. K.; Schubert, E. F. White light-emitting diodes: History, progress, and future. *Las. Photon. Rev.* **2017**, *11*, 1600147.

(4) Schubert, E. F.; Kim, J. K. Solid-State Light Sources Getting Smart. *Science* **2005**, *308*, 1274−1278.

(5) Kneissl, M. A Brief Review of III-Nitride UV Emitter Technologies and Their Applications. In *III-Nitride Ultraviolet*

DOI: 10.1021/acsenergylett.8b00002
ACS Energy Lett. 2018, 3, 655−662

Emitters; Kneissl, M., Rass, J., Eds.; Springer Series of Materials Science; Springer: Cham, Switzerland, 2016; Vol. *227*.
(6) Auf der Maur, M.; Pecchia, A.; Penazzi, G.; Rodrigues, W.; Di Carlo, A. Efficiency Droop in Green InGaN/GaN Light Emitting Diodes: The Role of Random Alloy Fluctuations. *Phys. Rev. Lett.* **2016**, *116*, 027401.
(7) Saito, S.; Hashimoto, R.; Hwang, J.; Nunoue, S. InGaN Light-Emitting Diodes on *c*-Face Sapphire Substrates in Green Gap Spectral Range. *Appl. Phys. Express* **2013**, *6*, 111004.
(8) Broell, M.; Sundgren, P.; Rudolph, A.; Schmid, W.; Vogl, A.; Behringer, M. New developments on high-efficiency infrared and InGaAlP light-emitting diodes at OSRAM Opto Semiconductors. *Proc. SPIE* **2014**, *9003*, 90030L.
(9) Kane, E. O. Band Structure of Indium Antimonide. *J. Phys. Chem. Solids* **1957**, *1*, 249−261.
(10) Harrison, W. A. The Energy Bands. In *Electronics Structure and Properties of Solids*; Harrison, W. A., Ed.; Dover Publications: New York, 1980.
(11) Zhang, Y.; Tan, Y.-W.; Stormer, H. L.; Kim, P. Experimental observation of the quantum Hall effect and Berry's phase in graphene. *Nature* **2005**, *438*, 201−204.
(12) Rinke, P.; Winkelnkemper, M.; Qteish, A.; Bimberg, D.; Neugebauer, J.; Scheffler, M. Consistent set of band parameters for the group-III nitrides AlN, GaN, and InN. *Phys. Rev. B: Condens. Matter Mater. Phys.* **2008**, *77*, 075202.
(13) de L. Kronig, R.; Penney, W. G. Quantum mechanics of electrons in crystal lattices. *Proc. R. Soc. London, Ser. A* **1931**, *130*, 499−513.
(14) Schubert, E. F. Shallow impurities. In *Doping in III−V Semiconductors*; Schubert, E. F., Ed.; Cambridge University Press: Cambridge, U.K., 1993.
(15) Schubert, E. F. Impurities in semiconductors. In *Physical Foundations of Solid-State Devices*; Schubert, E. F., Ed.; Rensselaer Polytechnic Institute: Troy NY, 2015.
(16) Alibert, C.; Bordure, G.; Laugier, A.; Chevallier, J. Electroreflectance and Band Structure of $Ga_xIn_{1-x}P$ Alloys. *Phys. Rev. B* **1972**, *6*, 1301−1310.
(17) Honda, M.; Ikeda, M.; Mori, Y.; Kaneko, K.; Watanabe, N. The energy of Zn and Se in $(Al_xGa_{1-x})_{0.52}In_{0.48}P$. *Jpn. J. Appl. Phys.* **1985**, *24*, L187−L189.
(18) Kasic, A.; Schubert, M.; Einfeldt, S.; Hommel, D.; Tiwald, T. E. Free-carrier and phonon properties of n- and p-type hexagonal GaN films measured by infrared ellipsometry. *Phys. Rev. B: Condens. Matter Mater. Phys.* **2000**, *62*, 7365−7377.
(19) Morkoç, H. General Properties of Nitrides. In *Handbook of Nitride Semiconductors and Devices*; Morkoç, H., Ed.; Wiley-VCH: Weinheim, Germany, 2008.
(20) Schöche, S.; Kühne, P.; Hofmann, T.; Schubert, M.; Nilsson, D.; Kakanakova-Georgieva, A.; Janzén, E.; Darakchieva, V. Electron effective mass in $Al_{0.72}Ga_{0.28}N$ alloys determined by mid-infrared optical Hall effect. *Appl. Phys. Lett.* **2013**, *103*, 212107.
(21) Silveira, E.; Freitas, J. A., Jr.; Kneissl, M.; Treat, D. W.; Johnson, N. M.; Slack, G. A.; Schowalter, L. J. Near-bandedge cathodoluminescence of an AlN homoepitaxial film. *Appl. Phys. Lett.* **2004**, *84*, 3501−3503.
(22) Piprek, J. AlGaN polarization doping effects on the efficiency of blue LEDs. *Proc. SPIE* **2012**, *8262*, 82620E.
(23) Simon, J.; Protasenko, V.; Lian, C.; Xing, H.; Jena, D. Polarization-induced hole doping in wide−band-gap uniaxial semiconductor heterostructures. *Science* **2010**, *327*, 60−64.
(24) Katsuragawa, M.; Sota, S.; Komori, M.; Anbe, C.; Takeuchi, T.; Sakai, H.; Amano, H.; Akasaki, I. Thermal ionization energy of Si and Mg in AlGaN. *J. Cryst. Growth* **1998**, *189-190*, 528−531.
(25) Neuschl, B.; Thonke, K.; Feneberg, M.; Goldhahn, R.; Wunderer, T.; Yang, Z.; Johnson, N. M.; Xie, J.; Mita, S.; Rice, A.; et al. Direct determination of the silicon donor ionization energy in homoepitaxial AlN photoluminescence two-electron transitions. *Appl. Phys. Lett.* **2013**, *103*, 122105.
(26) Stringfellow, G.; Craford, M. High brightness light emitting diodes. In *Semiconductors & Semimetals*; Willardson, R. K., Weber, E. R., Eds.; Academic Press: New York, 1997.
(27) Bhattacharyya, A.; Li, W.; Cabalu, J.; Moustakas, T. D.; Smith, D. J.; Hervig, R. L. Efficient p-type doping of GaN films by plasma-assisted molecular beam epitaxy. *Appl. Phys. Lett.* **2004**, *85*, 4956−4958.
(28) Park, J. H.; Kim, D. Y.; Hwang, S.; Meyaard, D.; Schubert, E. F.; Han, Y. D.; Choi, J. W.; Cho, J.; Kim, J. K. Enhanced overall efficiency of GaInN-based light-emitting diodes with reduced efficiency droop by Al-composition-graded AlGaN/GaN superlattice electron blocking layer. *Appl. Phys. Lett.* **2013**, *103*, 061104.
(29) Nam, K. B.; Nakarmi, M. L.; Li, J.; Lin, J. Y.; Jiang, H. X. Mg acceptor level in AlN probed by deep ultraviolet photoluminescence. *Appl. Phys. Lett.* **2003**, *83*, 878−880.
(30) Nakarmi, M. L.; Kim, K. H.; Khizar, M.; Fan, Z. Y.; Lin, J. Y.; Jiang, H. X. Electrical and optical properties of Mg-doped $Al_{0.7}Ga_{0.3}N$ alloys. *Appl. Phys. Lett.* **2005**, *86*, 092108.
(31) Chakraborty, A.; Moe, C. G.; Wu, Y.; Mates, T.; Keller, S.; Speck, J. S.; DenBaars, S. P.; Mishra, U. K. Electrical and structural characterization of Mg-doped p-type $Al_{0.69}Ga_{0.31}N$ films on SiC substrate. *J. Appl. Phys.* **2007**, *101*, 053717.
(32) Meyaard, D. S.; Lin, G.-B.; Cho, J.; Schubert, E. F.; Shim, H.; Han, S.-H.; Kim, M.-H.; Sone, C.; Kim, Y. S. Identifying the cause of the efficiency droop in GaInN light-emitting diodes by correlating the onset of high injection with the onset of the efficiency droop. *Appl. Phys. Lett.* **2013**, *102*, 251114.
(33) Shim, J.-I.; Han, D.-P.; Kim, H.; Shin, D.-S.; Lin, G.-B.; Meyaard, D. S.; Shan, Q.; Cho, J.; Schubert, E. F.; Shim, H.; et al. Efficiency droop in AlGaInP and GaInN light-emitting diodes. *Appl. Phys. Lett.* **2012**, *100*, 111106.
(34) Kioupakis, E.; Rinke, P.; Delaney, K. T.; Van de Walle, C. G. Indirect Auger recombination as a cause of efficiency droop in nitride light-emitting diodes. *Appl. Phys. Lett.* **2011**, *98*, 161107.
(35) Cho, J.; Schubert, E. F.; Kim, J. K. Efficiency droop in light-emitting diodes: Challenges and countermeasures. *Las. Photon. Rev.* **2013**, *7*, 408−421.
(36) Sun, W.; Shatalov, M.; Deng, J.; Hu, X.; Yang, J.; Lunev, A.; Bilenko, Y.; Shur, M.; Gaska, R. Efficiency droop in 245−247 nm AlGaN light-emitting diodes with continuous wave 2mW output power. *Appl. Phys. Lett.* **2010**, *96*, 061102.
(37) Kim, M.-H.; Schubert, M. F.; Dai, Q.; Kim, J. K.; Schubert, E. F.; Piprek, J.; Park, Y. Origin of efficiency droop in GaN-based light-emitting diodes. *Appl. Phys. Lett.* **2007**, *91*, 183507.
(38) Cao, X. A.; Yang, Y.; Guo, H. On the origin of efficiency roll-off in InGaN-based light-emitting diodes. *J. Appl. Phys.* **2008**, *104*, 093108.
(39) Verzellesi, G.; Saguatti, D.; Meneghini, M.; Bertazzi, F.; Goano, M.; Meneghesso, G.; Zanoni, E. Efficiency droop in InGaN/GaN blue light-emitting diodes: Physical mechanisms and remedies. *J. Appl. Phys.* **2013**, *114*, 071101.
(40) Wang, C. H.; Ke, C. C.; Lee, C. Y.; Chang, S. P.; Chang, W. T.; Li, J. C.; Li, Z. Y.; Yang, H. C.; Kuo, H. C.; Lu, T. C.; et al. Hole injection and efficiency droop improvement in InGaN/GaN light-emitting diodes by band-engineered electron blocking layer. *Appl. Phys. Lett.* **2010**, *97*, 261103.
(41) Ni, X.; Fan, Q.; Shimada, R.; Özgür, Ü.; Morkoç, H. Reduction of efficiency droop in InGaN light emitting diodes by coupled quantum wells. *Appl. Phys. Lett.* **2008**, *93*, 171113.
(42) Zhang, Y.; Krishnamoorthy, S.; Akyol, F.; Allerman, A. A.; Moseley, M. W.; Armstrong, A. M.; Rajan, S. Design and demonstration of ultra-wide bandgap AlGaN tunnel junctions. *Appl. Phys. Lett.* **2016**, *109*, 121102.
(43) Heera, V.; Panknin, D.; Skorupa, W. p-Type doping of SiC by high does Al implantation-problems and progress. *Appl. Surf. Sci.* **2001**, *184*, 307−316.
(44) Teukam, Z.; Chevallier, J.; Saguy, C.; Kalish, R.; Ballutaud, D.; Barbé, M.; Jomard, F.; Tromson-Carli, A.; Cytermann, C.; Butler, J. E.; et al. Shallow donors with high n-type electrical conductivity in

DOI: 10.1021/acsenergylett.8b00002
ACS Energy Lett. 2018, 3, 655−662

homoepitaxial deuterated boron-doped diamond layers. *Nat. Mater.* **2003**, *2*, 482−486.
(45) Park, J. H.; Cho, J.; Schubert, E. F.; Kim, J. K. The Effect of Imbalanced Carrier Transport on the Efficiency Droop in GaInN-Based Blue and Green Light-Emitting Diodes. *Energies* **2017**, *10*, 1277.
(46) Zhang, J.; Kuokstis, E.; Fareed, Q.; Wang, H.; Yang, J.; Simin, G.; Khan, M. A.; Gaska, R.; Shur, M. Pulsed atomic layer epitaxy of quaternary AlInGaN layers. *Appl. Phys. Lett.* **2001**, *79*, 925−927.
(47) Zhang, J. P.; Khan, M. A.; Sun, W. H.; Wang, H. M.; Chen, C. Q.; Fareed, Q.; Kuokstis, E.; Yang, J. W. Pulsed atomic-layer epitaxy of ultrahigh-quality $Al_xGa_{1-x}N$ structures for deep ultraviolet emissions below 230 nm. *Appl. Phys. Lett.* **2002**, *81*, 4392−4394.
(48) Brunner, F.; Protzmann, H.; Heuken, M.; Knauer, A.; Weyers, M.; Kneissl, M. High-temperature growth of AlN in a production scale 11 × 2" MOVPE reactor. *Phys. Status Solidi C* **2008**, *5*, 1799−1801.
(49) Chen, C. Q.; Zhang, J. P.; Gaevski, M. E.; Wang, H. M.; Sun, W. H.; Fareed, R. S. Q.; Yang, J. W.; Khan, M. A. AlGaN layers grown on GaN using strain-relief interlayers. *Appl. Phys. Lett.* **2002**, *81*, 4961−4963.
(50) Han, J.; Waldrip, K. E.; Lee, S. R.; Figiel, J. J.; Hearne, S. J.; Petersen, G. A.; Myers, S. M. Control and elimination of cracking of AlGaN using low-temperature AlGaN interlayer. *Appl. Phys. Lett.* **2001**, *78*, 67−69.
(51) Goepfert, I. D.; Schubert, E. F.; Osinsky, A.; Norris, P. E.; Faleev, N. N. Experimental and theoretical study of acceptor activation and transport properties in p-type $Al_xGa_{1-x}N$/GaN superlattice. *J. Appl. Phys.* **2000**, *88*, 2030−2038.
(52) Kim, J. K.; Waldron, E. L.; Li, Y.-L.; Gessmann, T.; Schubert, E. F.; Jang, H. W.; Lee, J.-L. P-type conductivity in bulk $Al_xGa_{1-x}N$ and $Al_xGa_{1-x}N/Al_yGa_{1-y}N$ superlattices with average Al mole fraction > 20%. *Appl. Phys. Lett.* **2004**, *84*, 3310−3312.
(53) Allerman, A. A.; Crawford, M. H.; Miller, M. A.; Lee, S. R. Growth and characterization of Mg-doped AlGaN-AlN short-period superlattices for deep-UV optoelectronic devices. *J. Cryst. Growth* **2010**, *312*, 756−761.
(54) Zheng, T. C.; Lin, W.; Liu, R.; Cai, D. J.; Li, J. C.; Li, S. P.; Kang, J. Y. Improve *p*-type conductivity in Al-rich AlGaN using multidimensional Mg-doped superlattices. *Sci. Rep.* **2016**, *6*, 21897.
(55) Carnevale, S. D.; Kent, T. F.; Phillips, P. J.; Mills, M. J.; Rajan, S.; Myers, R. C. Polarization-Induced pn Diodes in Wide-Band-Gap Nanowires with Ultraviolet Electroluminescence. *Nano Lett.* **2012**, *12*, 915−920.
(56) Schubert, M. F. Interband tunnel junctions for wurtzite III-nitride semiconductors based on heterointerface polarization charges. *Phys. Rev. B: Condens. Matter Mater. Phys.* **2010**, *81*, 035303.
(57) Growden, T. A.; Zhang, W.; Brown, E. R.; Storm, D. V.; Meyer, D. J.; Berger, P. R. Near-UV electroluminescence in unipolar-doped, bipolar-tunneling (UDBT) GaN/AlN heterostructures. *Light Sci. Appl.* **2018**, *7*, e17150.
(58) Takano, T.; Mino, T.; Sakai, J.; Noguchi, N.; Tsubaki, K.; Hirayama, H. Deep-ultraviolet light-emitting diodes with external quantum efficiency higher than 20% at 275 nm achieved by improving light-extraction efficiency. *Appl. Phys. Express* **2017**, *10*, 031002.
(59) Li, Y.-L.; Huang, Y.-R.; Lai, Y.-H. Investigation of Efficiency Droop Behaviors of InGaN/GaN Multiple-Quantum-Well LEDs with Various Well Thicknesses. *IEEE J. Sel. Top. Quantum Electron.* **2009**, *15*, 1128−1131.
(60) Feezell, D.; Schmidt, M.; DenBaars, S.; Nakamura, S. Development of Nonpolar and Semipolar InGaN/GaN Visible Light-Emitting Diodes. *MRS Bull.* **2009**, *34*, 318−323.
(61) Chakraborty, A.; Haskell, B. A.; Keller, S.; Speck, J. S.; DenBaars, S. P.; Nakamura, S.; Mishra, U. K. Nonpolar InGaN/GaN emitters on reduced-defect lateral epitaxially overgrown *a*-plane GaN with drive-current-independent electroluminescence emission peak. *Appl. Phys. Lett.* **2004**, *85*, 5143−5145.
(62) Feezell, D. F.; Speck, J. S.; DenBaars, S. P.; Nakamura, S. Semipolar $(20\bar{2}1)$ InGaN/GaN Light-Emitting Diodes for High-Efficiency Solid-State-Lighting. *J. Disp. Technol.* **2013**, *9*, 190−198.
(63) Kashima, Y.; Maeda, N.; Matsuura, E.; Jo, M.; Iwai, T.; Morita, T.; Kokubo, M.; Tashiro, T.; Kamimura, R.; Osada, Y.; et al. High external quantum efficiency (10%) AlGaN-based deep-ultraviolet light-emitting diodes achieved by using highly reflective photonic crystal on p-AlGaN contact layer. *Appl. Phys. Express* **2018**, *11*, 012101.
(64) Kim, D. Y.; Park, J. H.; Lee, J. W.; Hwang, S.; Oh, S. J.; Kim, J.; Sone, C.; Schubert, E. F.; Kim, J. K. Overcoming the fundamental light-extraction efficiency limitations of deep ultraviolet light-emitting diodes by utilizing transverse-magnetic-dominant emission. *Light: Sci. Appl.* **2015**, *4*, e263.
(65) Lee, J. W.; Kim, D. Y.; Park, J. H.; Schubert, E. F.; Kim, J.; Lee, J.; Kim, Y.-I.; Park, Y.; Kim, J. K. An elegant route to overcome fundamentally-limited light extraction in AlGaN deep-ultraviolet light-emitting diodes: Preferential outcoupling of strong in-plane emission. *Sci. Rep.* **2016**, *6*, 22537.
(66) Lee, J. W.; Park, J. H.; Kim, D. Y.; Schubert, E. F.; Kim, J.; Lee, J.; Kim, Y.-I.; Park, Y.; Kim, J. K. Array of Truncated Cone AlGaN Deep-Ultraviolet Light-Emitting Diodes Facilitating Efficient Outcoupling of in-Plane Emission. *ACS Photonics* **2016**, *3*, 2030−2034.

DOI: 10.1021/acsenergylett.8b00002
ACS Energy Lett. 2018, 3, 655−662